

On the Detonation Pressure Produced at the Inner Surface of the Charge Hole

By

Ichiro ITO* and Kōichi SASSA*

(Received October 22, 1960)

In these experimental studies, the magnitude of the detonation pressure produced at the inner surface of the charge hole by the detonation of a confined explosive and the change in that pressure with time were chiefly investigated by means of measuring the stress wave produced within a steel rod by this explosion, utilizing a specially designed piezo-electric pressure gauge. The main element of the above pressure gauge was a transducing unit which contains a barium titanate ceramic transducer enclosed tightly in the gauge body. The strong stress caused by the explosion must be properly reduced before being imposed upon the transducing unit. In this gauge such reduction of stress was accomplished by placing an ebonite directly on top of the upper surface of the ceramic transducer.

The results obtained are briefly shown below. In the case of the detonation of a confined 45g- or 90g-cartridge charged in a bore hole with a charging density of 0.7 g/cm^3 , the rise time to the peak pressure was less than about $2\mu\text{s}$, and this peak pressure decreased rapidly to the state of so-called static pressure about $15\mu\text{s}$ later, decreasing very slowly thereafter. The duration time of such detonation pressure in the charge hole was about half a millisecond in these experiments.

The value of about $3 \times 10^4 \text{ kg/cm}^2$ was obtained as the steady detonation pressure (generally known as P_{G-T}) of a 45g-cartridge of No. 3 Take dynamite under our experimental conditions, corresponding to a velocity of detonation of 3,300 m/s.

Introduction

In order to investigate the mechanism of rock blasting, it is considered to be very important to know the magnitude of the pressure produced at the inner surface of the charge hole by the detonation of a confined explosive and also to know the change in that pressure with time. Therefore, we recently devised a specially designed piezo-electric pressure gauge. By means of this pressure gauge, the strong stress wave produced within a steel rod (a gauge head) by the detonation of an explosive which was placed in contact with this rod in the charge hole was measured, and on the other hand, the stress wave produced

* Department of Mining Engineering

within the steel rod by the detonation of the same explosive fired freely in air was also measured.

As the result of comparing the magnitudes of these two stress waves, the ratio of the increase of the detonation pressure caused by the effect of confinement was estimated. Furthermore, by means of considering the stress wave shape in the steel rod and the collision effect of the detonation wave against a solid material, the magnitude of the pressure on the inner surface of the charge hole and the change in that pressure with time were investigated.

Piezo-electric Gauge

The piezo-electric pressure gauge devised to measure the strong stress wave in a steel rod consists of the following four parts; a gauge head, a gauge body, a press screw with a hexagonal cavity, and the transducing unit which contains a barium titanate ceramic transducer and an ebonite. The construction of this gauge is shown schematically in Fig. 1.

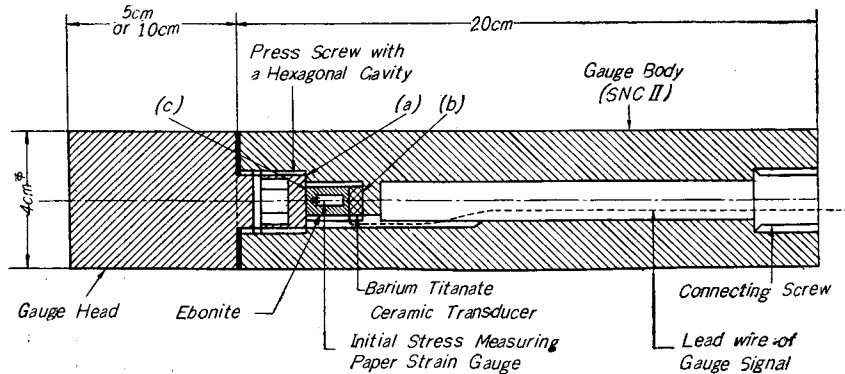


Fig. 1. Construction of the piezo-electric gauge.

As shown in Fig. 1, the principle of this gauge is to measure the strain produced in the gauge body by the stress wave travelling along its axis by means of the piezo-electric transducer. So, it is important that the strain in the gauge body be transmitted exactly to the transducing unit in every case. Therefore, the transducing unit must be enclosed tightly in the gauge body. In order to satisfy this condition, the press screw must be screwed firmly into the gauge body and the face (c) of the press screw ought to press tightly on edge (a) of the gauge body*, thus forming a compartment for the transducing unit between face (c) of the press screw and the inner surface (b) of the gauge body. As the transducing unit is made to be about 0.15 mm longer than the length of the

* The force acting between face (c) and face (a) is about 3,000 kg.

transducing unit compartment, the unit can be enclosed tightly therein. Under normal use, an initial stress of 400 kg/cm^2 , which is measured by two paper strain gauges cemented on the ebonite surface, is expected to be imposed upon the unit.

Now, let us denote the acceleration of the displacement of face (b) as α , the mass of the piezo-electric transducer as m , and the initial force acting on the piezo-electric transducer as F_0^* . Then, if the condition $F_0/m \geq \alpha$ is satisfied, the piezo-electric transducer will follow exactly the displacement of face (b) without being separated. Therefore, F_0/m determines the critical acceleration of the displacement of face (b). As that value of F_0/m , an acceleration of $1.8 \times 10^8 \text{ cm/sec}^2$ was obtained for this gauge. Similarly, for the critical acceleration of face (c), a value of $2.7 \times 10^8 \text{ cm/sec}^2$ was obtained. However, the effects of gravity and the viscosity of the ebonite were neglected in these considerations.

Accordingly, if the acceleration of the displacement which is produced in the gauge body by the propagation of the stress wave is smaller than the above critical values, the stress wave can be measured exactly by this gauge. In our experiments, this condition was satisfied in every case.

The gauge body and the press screw are made from heat-treated nickel chrome steel. The stress-strain diagrams for the nickel chrome steel, the barium titanate ceramics and the ebonite are shown in Figs. 2, 3 and 4 respectively, each of which was determined by statical compression tests in a testing machine. As to the barium titanate ceramics, as shown in Fig. 3, the stress-strain relationship is linear only within the stress range less than 800 kg/cm^2 . It is usually desirable for accuracy of measurement to stay within the elastic limit of the material used. Therefore, in order to measure high pressures, like the detonation pressure, the pressure acting on the barium titanate ceramics must be reduced to about 800 kg/cm^2 .

In the case of this gauge, the pressure acting on the barium titanate transducer is reduced by using the difference of Young's moduli in two materials.

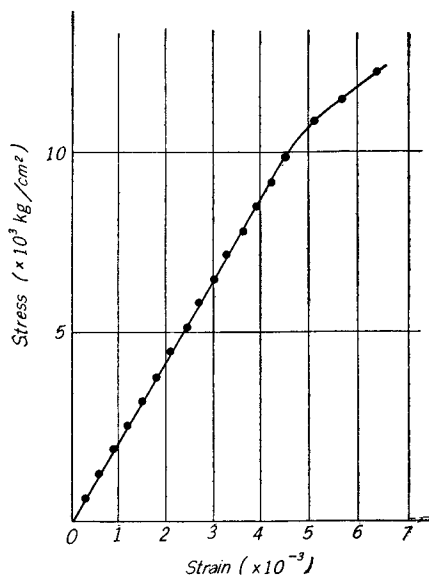


Fig. 2. Stress-strain diagram for nickel chrome steel.

* $F_0 = (\text{the initial stress in the transducing unit}) \times (\text{the cross sectional area of the transducing unit})$

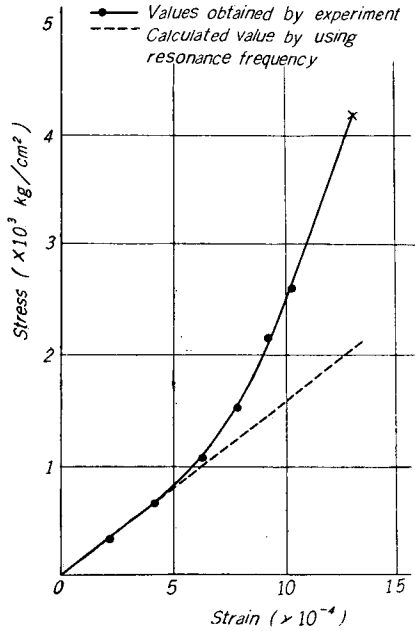


Fig. 3. Stress-strain diagram for barium titanate ceramics.

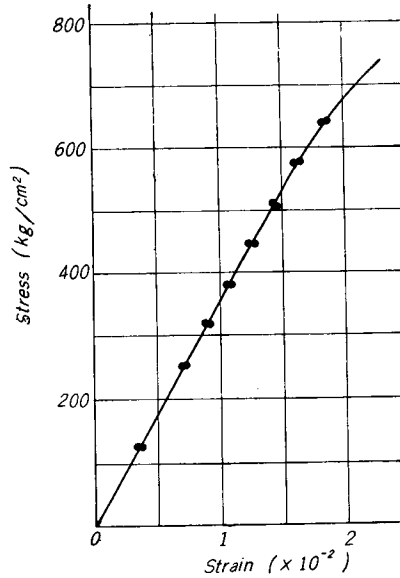


Fig. 4. Stress-strain diagram for ebonite.

Now, let us consider a body composed of two materials *A* and *B*, where the material *B* is tightly enclosed within material *A* as shown in Fig. 5. When this body is subjected to a force acting as indicated by the arrow in the figure, the induced strain must be equal in the two materials. Consequently the following equation is obtained,

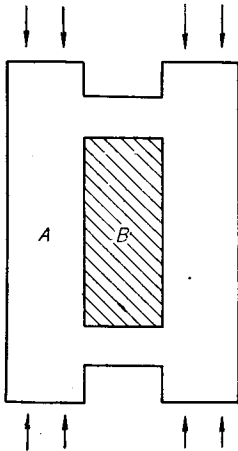


Fig. 5. A schematic model composed of two materials.

$$\sigma_B = \frac{E_B}{E_A} \cdot \sigma_A \quad \dots\dots\dots(1)$$

where σ_A , E_A and σ_B , E_B indicate the induced stresses and Young's moduli of the materials *A* and *B* respectively. Therefore, in the case where E_B is less than E_A , σ_B becomes smaller than σ_A . In our gauge, the gauge body and the ebonite may correspond respectively to the materials *A* and *B*. Now if we denote the stresses produced within the gauge body and the ebonite as $\sigma_{S.N.C.}$ and σ_{ebonite} respectively, then the relation between them is

$$\sigma_{S.N.C.} = 40 \cdot \sigma_{\text{ebonite}} \cdot \dots\dots\dots(2)$$

But in this calculation, the strain in the barium titanate ceramics is neglected and the static Young's modulus is

adopted. Therefore, the stress produced within the barium titanate ceramic transducer becomes about 1/40 as compared with the axial stress produced within the gauge body. However, the dynamic Young's modulus is generally thought to be several times greater than the static one¹⁾. Consequently the maximum limit of the pressure which we can measure accurately by this piezo-electric gauge is also supposed to be greater than the value which is determined by using the static Young's modulus.

The barium titanate ceramic transducer used in this gauge is a circular disk 3 mm in thickness and 8 mm in diameter, and its axis of polarization is parallel to that of the disk.

The relation between the force F acting on the barium titanate ceramic transducer and the amount of electricity Q produced within it is generally known as

$$Q = d \times F \quad \dots\dots\dots(3)$$

where d denotes the piezo-electric modulus. The value of d is 570×10^{-8} esu/dyne for barium titanate ceramics, so equation (3) can be written as follows.

$$Q_{(e.s.u.)} = 5.7 \times 10^{-6} F_{(dyne)} \quad \dots\dots\dots(4)$$

or

$$Q_{(\mu C)} = 1.86 \times 10^{-3} F_{(kg)} \quad \dots\dots\dots(5)$$

The response characteristics of the barium titanate ceramic transducer used in this gauge were measured by a drop test. The initial stress is always imposed upon the transducer which is enclosed in the gauge body, and therefore when the gauge body is strained by the stress wave, the transducer receives both the initial stress and the dynamic stress which is produced by the stress wave. Therefore, in testing the response characteristics, an impulsive loading was applied to the barium titanate ceramic transducer, under conditions the same as when it is enclosed in the gauge body. An example of the response characteristics obtained in these tests is shown in Fig. 6. In these measurements, both the initial stress and the dynamic stress produced within the transducer by the impulsive loading were measured by two paper strain gauges affixed to the surface on opposite sides of a steel column. The diameter of this steel column

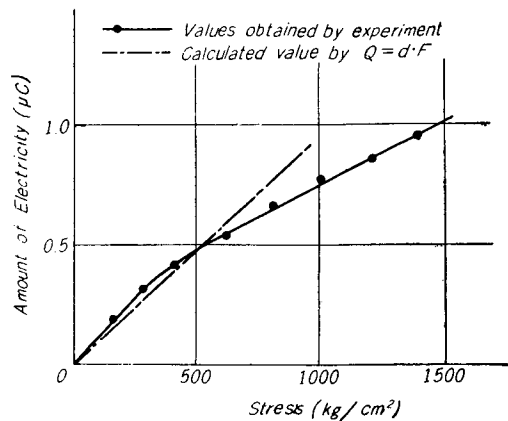


Fig. 6. Response characteristic for the barium titanate ceramic transducer.

was made equal to that of the transducer, and it was placed in contact with the transducer.

The pressure calibration of this gauge was carried out as follows. The gauge head having a length 10 cm was attached to the gauge body, and it was struck by an explosion of a detonator of No. 6 strength in the first test and by an explosion of a 45g-cartridge of No. 3 Take dynamite in the second test, each being placed in contact with the gauge head along its axis. In each test the amount of electricity (i.e. the gauge signal) under these impulsive loadings was measured.

On the other hand, the magnitude of the peak stress in such stress waves was measured in accordance with the following principle*. Generally when a bar specimen is struck at one end by an impulsive loading, a compression stress wave is generated and propagated along the axis of the bar. In this case, it is well known that the stress σ at any point in the bar specimen can be represented by the following equation,

$$\sigma = \rho \cdot c \cdot v \quad \dots\dots\dots(6)$$

where ρ is the density of the specimen, c is the velocity of propagation of the stress wave in the specimen, and v is the particle velocity in the stress wave. Accordingly, the magnitude of the stress at any point in the specimen can be calculated by measuring the magnitudes of ρ , c and v .

Now in order to obtain the same stress waves as those obtained in the above experiments, a specimen was made from the same material and of the same size as the gauge head (4 cm in diameter and 12.8 cm in length). Then one end of this specimen was struck by an explosion either of a detonator of No. 6 strength or of a 45g-cartridge of No. 3 Take dynamite, and at the other end the particle velocity in the stress wave was measured by a method similar to that used by Rinehart and others²⁾. At the same time, the time required for the stress wave to propagate between two known marks on the specimen was measured in order to obtain the velocity of propagation of the stress wave in the specimen. Thus in these experiments the stress values of 2,800 kg/cm² and 8,000 kg/cm² were established as the peak stress values corresponding to the gauge signals obtained previously.

In this way, the present piezo-electric gauge was calibrated by means of two known stress waves and by the measured response characteristics of the barium titanate ceramic transducer.

* Hereafter the stress measurement based on this principle shall provisionally be called the pellet method.

Moreover, in these experiments, the stress wave shapes obtained by using the piezo-electric gauge were compared with those determined by the pellet method, and it was found that the stress wave produced in the side wall of the transducing unit compartment can be traced exactly by this gauge.

Experimental Procedure

The general arrangement of the experiment for measuring the stress wave produced within a steel rod (the gauge head) by the detonation of an explosive in a charge hole, is shown in Fig. 7. A bore hole having a depth of about 70 cm was drilled downward with an inclination of about 45° by a bit with 55 mm gauge. The rocks surrounding the bore hole were a kind of serpentine. No. 3 Take dynamite was used as the explosive, and the velocity of detonation of this explosive under complete confinement is reported to be 5,500 m/s. The composition of this explosive is shown in Table 1.

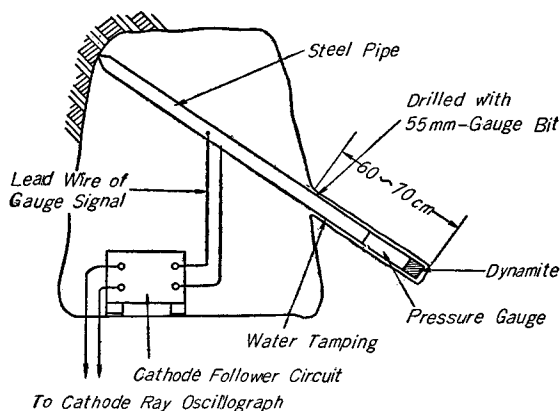


Fig. 7. General experimental arrangement for the experimental condition of group (B).

Table 1
Composition of No. 3 Take Dynamite (per cent. by weight)

Nitroglycerine gel	Ammonium nitrate	Other materials
16~20	65~75	10~20

The more detailed arrangement of the gauge and the explosive is shown in Fig. 8. The gauge head, whose length was either 10 cm or 5 cm, was screwed on to the gauge body and a 45g- or 90g-cartridge of No. 3 Take dynamite, shaped to about 35 mm in diameter, was placed in tight contact with the end of the gauge head. Both the explosive and the gauge head were covered with an iron pipe of 0.5 mm in thickness, and thereafter a lump of clay was packed into the iron pipe. The gauge and the explosive, thus set up, were inserted into the bore hole as shown in Fig. 7, and the open space between the gauge and the inner surface of the bore hole was filled with water. Thus the explosive was confined with a charging density of about 0.7 g/cm³.

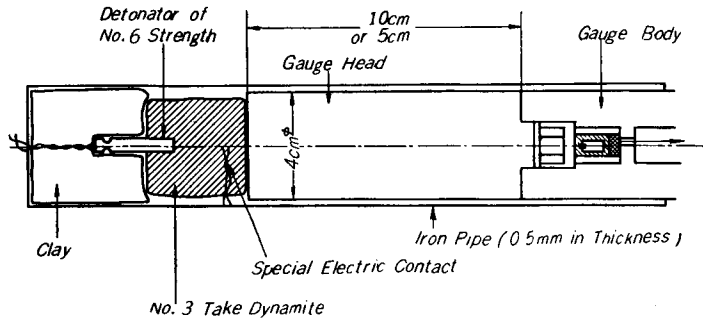


Fig. 8. Detailed sketch of the arrangement of gauge and explosive.

In order to prevent distortion of the recorded wave pattern by the arrival of reflected stress waves produced at the rear end of the gauge, a thick steel pipe, about 2 m long with inside and outside diameters of 15 mm and 34 mm respectively, was attached to the rear end of the gauge body.

The explosive was detonated by a detonator of No. 6 strength, and in order to catch the instant of detonation a special electric contact was used. This contact is composed of fine insulated wires twisted together, the top of which is cut to make a tiny gap and pushed into the explosive as shown in Fig. 8. When the explosive is detonated, ionized gases are produced around the gap of these insulated wires, therefore the circuit containing this electric contact is closed at the instant of the arrival of the detonation wave. By utilizing this contact, the recording apparatus was synchronized to the instant of the detonation.

The general arrangement of the signal recording apparatus is shown in Fig. 9. A piezo-electric crystal produces the electric charge on each pole corresponding to a strain in the crystal. Accordingly, in the case of the pressure measurement using the piezo-electric transducer, the time constant of the circuit* which contains

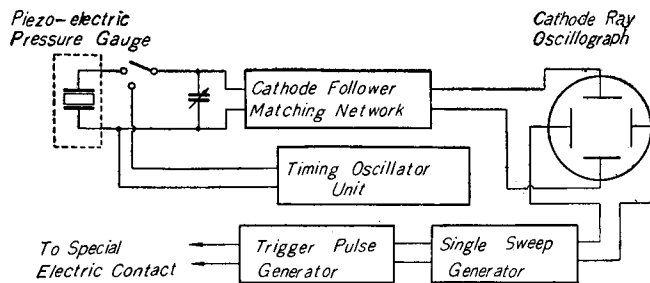


Fig. 9. General arrangement of the signal recording apparatuses.

* In these experiments, this time constant was about 30 ms, therefore it was much longer than the duration time of the phenomena measured.

the piezo-electric transducer must be much longer than the duration time of the phenomena measured. Consequently, the circuit which contains the piezo-electric transducer becomes a high impedance circuit. On the other hand, the gauge signal must be transmitted a distance of at least 50 m from the gauge to the recording unit in the case of experiments on blasting, and therefore in order to avoid noises from the line, the gauge signal must be transmitted in a low impedance line.

Accordingly, in these experiments, a cathode follower matching network was placed near the piezo-electric gauge and by this network the line impedance was lowered to about 90Ω , and the signal was transmitted by this low impedance line. Therefore few disturbances due to line noises were encountered in these experiments.

The frequency characteristic of the signal recording circuit, including the line of the signal transmission, is shown in Fig. 10.

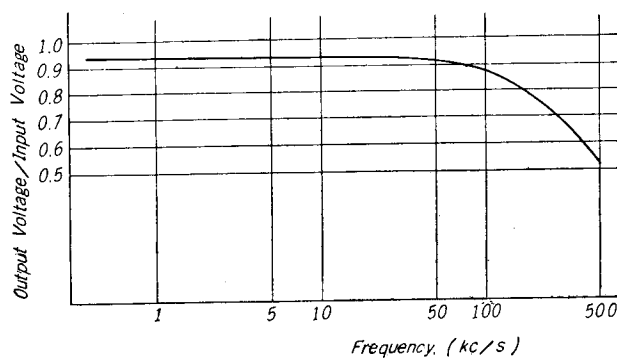


Fig. 10. Frequency characteristic of signal recording circuit.

The measurements of the stress wave in a steel rod attacked by the detonation of an explosive were performed under the following four conditions. The four conditions are divided into two parts.

- (A): The first part (hereafter indicated as experimental condition (A)) was the impact by the explosive which was detonated without confinement, namely, the gauge head having the length of 10 cm was affixed to the gauge body, and this gauge head was struck freely in air by the detonation of a 45 g-cartridge of No. 3 Take dynamite which was set up in contact with the end of this gauge head. Accordingly, the measured stress wave under this condition corresponds to the stress wave at the point 12.8 cm distant from the shot point.
- (B): The second part was the impact by an explosive which was detonated in a bore hole, as shown in Figs. 7 and 8. Moreover, this second part

could be divided into the following three conditions which are itemized simply below ;

- (B-1): 45g-cartridge of No. 3 Take dynamite was used.
The stress wave was measured at the point 12.8 cm distant from the shot point.
- (B-2): 90g-cartridge of No. 3 Take dynamite was used.
The stress wave was measured at the point 12.8 cm distant from the shot point.
- (B-3): 45g-cartridge of No. 3 Take dynamite was used.
The stress wave was measured at the point 7.8 cm distant from the shot point.

General Characteristics of the Stress wave Shape

An example of the pressure-time traces for the stress waves in the steel rod obtained under experimental condition (A) is shown in Fig. 11. The rise time of

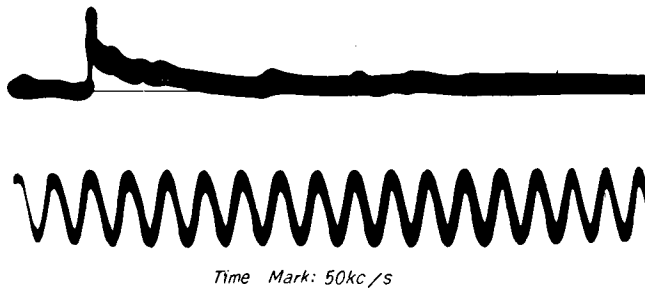


Fig. 11. Typical pressure-time trace for the stress wave obtained under experimental condition (A).

the stress at the front of this stress wave was about $2\mu s$, and also the duration time of the stress ranged from about $70\mu s$ up to $100\mu s$. Therefore, the wave length of this stress wave was about 50 cm. The semilogarithmic plots of the pressure ratio against time for the stress wave obtained under the experimental condition (A) are shown in Figs. 12 and 13. The plotted points in Fig. 12 are approximately linear, therefore the relation between stress and time under experimental condition (A) can be approximately represented as follows

$$P_t = A \cdot P_{max} \cdot \log t + B \quad (t_0 < t < t_1) \quad \dots\dots\dots (7)$$

where A and B are constants. Furthermore, the sharp wave shape near the wave front, as will be explained later in detail, may be formed by the effect of a pressure increase at the shot point caused by the collision of the detonation wave against the gauge head. If the pressure increase caused by this effect is reasonably

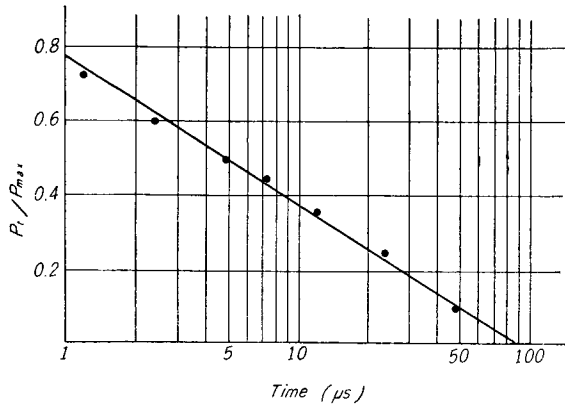


Fig. 12. Semilogarithmic plot of pressure ratio against time obtained under experimental condition (A).

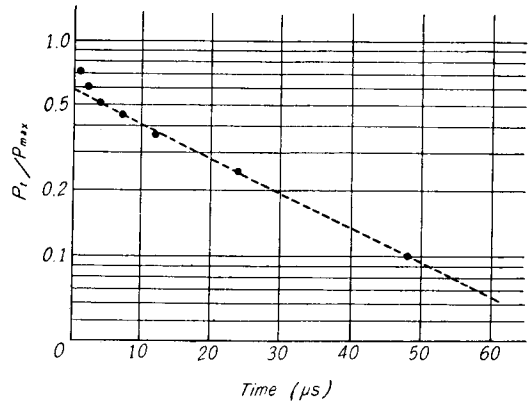


Fig. 13. Another semilogarithmic plot of pressure ratio against time obtained under experimental condition (A).

corrected, the relation between pressure and time will be represented by a dotted line such as is shown in Fig. 13 and can be approximated by the form

$$P_t = P_{max} \cdot e^{-\alpha t} \quad (t_0 < t < t_1) \quad \dots\dots\dots(8)$$

where α is a constant. The wave shape thus corrected is thought to indicate the general shape of the detonation wave derived from an explosive fired freely in air.

Next, let us consider the stress wave shape obtained under the experimental conditions in group (B). No remarkable differences among the stress wave shapes obtained under the experimental conditions (B-1), (B-2) and (B-3) could be found in the present experiments. An example of the pressure-time traces for the stress waves obtained under these experimental conditions is shown in Fig. 14. Fig. 15 shows a simplified trace which was copied carefully so as not to miss the dominant characteristics which appeared in the original.

In each case under these experimental conditions where water tamping is adopted, the gauge body, which is being kept in a condition of uni-axial compression by the stress wave propagated along its axis, is suddenly thrown into a condition of tri-axial compression when it is subjected to the additional side pressure generated by the arrival of the shock wave which is projected into the water by the explosion. Accordingly, the distortion in the wave shape caused by this side pressure must be corrected. The velocity of propagation of the shock wave produced in the water by the explosion under these experimental conditions may be considered to be about 2,000 m/s³. Therefore the arrival of the shock wave through the tamping water to the side wall of the transducing

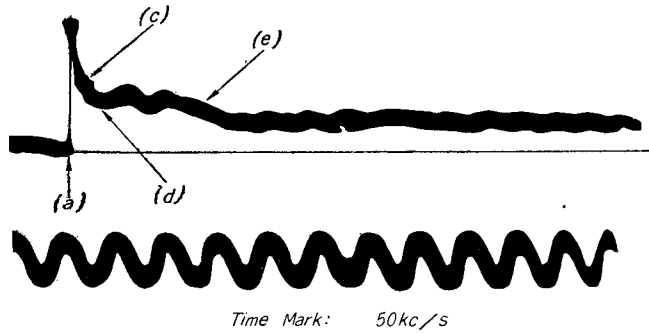


Fig. 14. Typical pressure-time trace for the stress wave obtained under experimental condition of group (B).

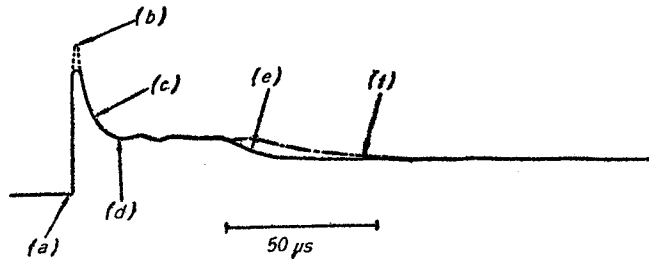


Fig. 15. Simplified trace copied from the original trace.

unit compartment will be delayed about $40\mu s$ compared with the arrival of the stress wave through the gauge head. Therefore, it may be considered that the comparatively rapid pressure decrease indicated by the mark (e) on the pressure-time traces shown in Figs. 14 and 15 is produced by the effect of the side pressure on the gauge body by the arrival of the shock wave through the water. Consequently, in order to obtain the real stress wave shape under these experimental conditions, this pressure decrease must be corrected by considering the shock wave shape acting on the side wall of the gauge. The corrected relation of pressure and time near point (e) is indicated by the chain line in Fig. 15. Thereafter, the side wall of the gauge body is also compressed by expansion of the produced gases, but these gases are considered to expand very slowly, and therefore the effects upon the gauge caused by expansion of these gases may be neglected in these experiments.

Next, the rapid rise and fall of the stress near the peak corresponds to a frequency of about 150 kc/s , and therefore the wave shape near the peak must be corrected according to the frequency characteristic of the recording circuit. This correction resulted in the dotted line shown in Fig. 15.

On the corrected stress wave shape shown in Fig. 15, the rise time of the

stress (the time required between points (a) and (b)) is about $2\mu\text{s}$, accordingly it is almost equal to that under experimental condition (A). The time required between points (a) and (c) is about $5\mu\text{s}$, and the magnitude of the stress at point (c) is about one half of that at point (b). The time required between points (a) and (d) is about $12\mu\text{s}$ and the magnitude of the stress at point (d) is about one third of that at point (b). These peculiar points (c) and (d) were also noticed in the wave shape obtained under experimental condition (A). Furthermore, it may be considered that the sharp wave shape near the wave front, that between points (a) and (c), is mainly influenced by the dynamic properties of the explosive (velocity of detonation, brisance and etc.) and by the dynamic character of the attacked material (characteristic impedance), as will be explained later. Beyond point (d) the stress decreases very slowly, and this part of the stress wave does not appear in the stress wave under experimental condition (A). Therefore, it is evident that this part of the stress wave is generated by the interruption of the expansion of the gases produced within the charge hole. Consequently, the duration time of this phase is influenced by the amount of explosive, the static properties of the explosive and the effect of tamping. That duration time was about $500\mu\text{s}$ in these experiments. The stress beyond point (d) decreases very slowly, but it decreases even more slowly beyond point (f). The time required from point (a) to point (f) is about $100\mu\text{s}$ and the magnitude of the stress at point (f) is about one half of that at point (d).

Peak Stress Values

From the results obtained in the experiments under the above four conditions, the peak stress values in the measured stress waves were calculated and are shown in Table 2 together with the ratios between these calculated peak pressures.

As shown in the table, the peak stress value obtained under experimental condition (B-1) was 1.5 times as large as that obtained under experimental condition (A). As the causes for this increase in the peak stress, the following two factors may be considered, namely;

- (1) The increase in the peak stress which is caused by the pressure increase of the detonation wave itself related to the increase of the velocity of detonation under a confined condition.
- (2) The detonation near the initial point of ignition in the explosive may project a shock wave into the narrow gap between the explosive and the iron pipe which covers the explosive and the gauge head. The arrival of this shock wave at the gauge head is thought to be almost simultaneous with the arrival of the detonation wave itself. Accordingly, the super-

position of this shock wave on the detonation wave at the gauge head is thought to be another factor which causes the increase of the peak stress.

In order to study which of these two factors has a greater influence upon the increase in the peak stress, the increase of the pressure at the detonation wave front in relation to the increase of the velocity of detonation must be investigated under these experimental conditions. Therefore, in the first place, the velocities of detonation of the respective explosives under these experimental conditions were measured by measuring the time required for the detonation wave to propagate between two known marks which were formed by the special electric contact explained before. As the result of these measurements, the velocities of 2,800 m/s, 3,300 m/s and 3,500 m/s were obtained as the velocities of detonation, corresponding to the experimental conditions (A), (B-1) and (B-2) respectively. Next, the increase of the pressure at the detonation wave front in relation to the increase of the velocity of detonation was measured as follows. A steel disk having a thickness of 5 mm was struck by the detonation of a 45-g or 90-g-cartridge of No. 3 Take dynamite which was placed tightly in contact with one end of this steel disk, and then the peak stress values at the other end of the disk were measured and calculated by using the pellet method. At the same

Table 2
Peak Stress Values in the Stress Waves produced in a Steel Rod

Experimental Condition	Peak Stress Value in the Stress Wave (kg/cm ²)	Mean Value of the Peak Stress (kg/cm ²)	Ratio between Peak Stress Values	
(A)	9,000 6,000 11,000 9,000 6,000 6,000 8,000 9,000	8,000	1.0	
(B-1)	11,000 13,000 13,000 12,000 12,000 15,000 14,000 9,000	12,000	1.5	1.0
(B-2)	14,000 19,000 14,000 15,000 17,000	16,000	2.0	1.3
(B-3)	17,000 15,000	16,000	2.0	1.3

time, the velocity of the detonation wave which struck the steel disk was also measured. Thus the peak stress values corresponding to the respective velocities of detonation were obtained. The results are shown in block in Table 3.

The effect due to the amount of explosive may be included in the results shown in Table 3, but so far as the magnitude of the pressure at the detonation wave front is concerned, it is mainly influenced by the velocity of detonation and the density of explosive rather than by the amount of explosive. Therefore, the increase of the stress shown in this table may be considered to be due to the increase of the velocity of detonation. Accordingly, the increase of the peak stress under experimental condition (B-1) in the former experiments may also be largely attributed to the increase of the velocity of detonation.

Table 3
Peak Stress Values produced in a Steel Rod at the Point 5 mm distant from the Attacked Point and the Velocity of Detonation

Explosive	Amount of Explosive (g)	Velocity of Detonation (m/s)	Peak Stress Value (kg/cm ²)	Ratio between Peak Stress Value
No. 3 Take Dynamite	45	2,800	35,000	1.0
	90	3,300	48,000	1.37

Furthermore, it can be surmised that the value of the peak pressure at the detonation wave front may increase more and more up to the value corresponding to the maximum velocity of detonation of the explosive which is obtained by the detonation under the complete confinement.

The peak stress value in the stress wave obtained under experimental condition (B-2) was 1.3 times as large as that in the case of (B-1). The cause of this increase in the peak stress may be considered to be due to two factors explained previously.

Further Consideration on the Stress Wave Shape

The features of the stress waves produced within a steel rod under an explosion's attack in a bore hole have already been mentioned above, and next let us consider the physical meaning which the so-called peculiar points in the stress wave shapes possess, by referring to the theory of the shock wave. The detonation wave may be regarded as a kind of a shock wave sustained by the heat of reaction, so the theory of the shock wave is applicable.

Now if we assume that D denotes the velocity of a shock wave, P_0 , V_0 and P , V denote the pressures and the specific volumes in the front and in the rear of the shock wave front respectively, and W denotes the particle velocity, then

the following well-known relations, are obtained for a one-dimensional plane shock wave,

$$D = V_0 \sqrt{\frac{(P - P_0)}{(V_0 - V)}} \dots\dots\dots(9)$$

$$W = \sqrt{(V_0 - V)(P - P_0)} \dots\dots\dots(10)$$

Consequently when a detonation wave of pressure at the wave front, P_1 , particle velocity, W_1 , and specific volume V_1 impinges on a solid material of pressure P_0 in which the specific volume is V_0 , if the pressure and particle velocity at the boundary turn into P_2 and W_2 and also the specific volumes of the solid material and the detonation products at the boundary turn into V_0' and V_1' respectively, the following relations are obtained by applying equation (10) at this boundary.

As to the shock wave produced in the solid material:

$$W_2 = \sqrt{(P_2 - P_0)(V_0 - V_0')} \dots\dots\dots(11)$$

As to the shock wave reflected back into the detonation products:

$$W_1 - W_2 = \sqrt{(P_2 - P_1)(V_1 - V_1')} \dots\dots\dots(12)$$

Accordingly, by plotting the possible relations between pressure and particle velocity for the two shock waves indicated in the above equations, the pressure produced at the boundary is obtained at the intersection of these two curves.

To estimate the pressure produced at the boundary in accordance with the above principle, the relation between pressure and particle velocity in the shock wave reflected back into the detonation products was calculated for TNT and Tetryl depending upon the theoretical study of detonation phenomena made by T. Hikita⁴⁾. As to the state of solid materials at higher pressures, the experimental results for some solid materials obtained by I. Itō and T. Sakurai⁵⁾ are quoted here. The results obtained in this way are shown in Fig. 16. The coordinates of the right-end points in the curves for TNT and Tetryl in Fig. 16, indicate the pressures and the particle velocities at the C-J

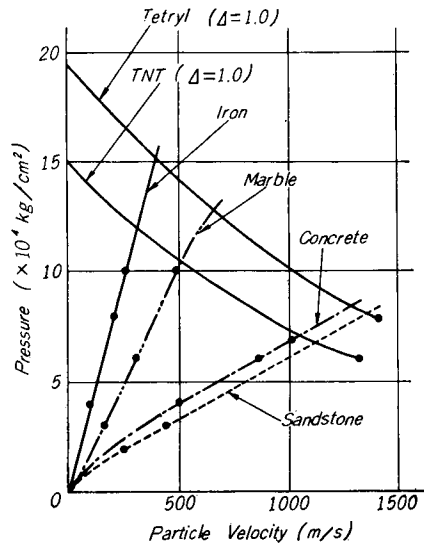


Fig. 16. Relation between pressure and particle velocity for some kinds of explosives and solid materials.

planes* in the detonation waves for TNT and Tetryl, and also the tangents of P - W curves for the solid materials represent the characteristic impedances of each material. The ratios of the pressures produced at the boundary to the pressures at the C - J planes in the detonation waves for TNT and Tetryl were calculated for some solid materials shown in Fig. 16 and the results are shown in Table 4. But in these considerations, the magnitudes of the pressure and the particle velocities in these impinging detonation wave fronts were assumed to be those at the C - J planes. As shown in Table 4, it is clearly understood that the magnitude of pressure at the boundary is influenced by the dynamic characteristics of the attacked material and of the explosive and also by the pressure at the detonation wave front. In the case of iron, the peak pressure produced at the attacked surface reaches a value about twice as large as the magnitude of the pressure at the detonation wave front.

Table 4
Ratios between the Pressure at the Attacked Surface of Some Materials and the Pressure at the Detonation Wave Fronts

Attacked Material	Density (g/cm ³)	TNT ($\Delta=1.0$ g/cm ³) $D=4,850$ m/s*	Tetryl ($\Delta=1.0$ g/cm ³) $D=5,400$ m/s*
Iron	7.86	2.01	1.98
Marble	2.7	1.74	1.65
Concrete	1.97	1.17	1.06
Sandstone	2.4	1.10	1.03

* Calculated value

Moreover, it must be added that these pressure increases produced at the boundary due to the collision of the detonation wave against solid materials have been studied by many investigators and their recent results have kindly been summarized in the paper written by F. W. Brown⁶.

Next, referring to the hydrodynamic theory of detonation, let us consider the features in the shape of the stress wave within a steel rod produced by the impact of the detonation wave.

According to the hydrodynamic theory of detonation as shown in Fig. 17, a very thin shock zone, the thickness of which is considered to be about 10^{-5} cm, exists in front of a reaction zone and the sudden increases in pressure and temperature and the comparatively slight increase in density occur in this shock zone. The explosive then undergoes chemical decomposition at the end of the shock zone. The chemical reaction finishes completely at the C - J plane where

* The C - J plane denotes a plane satisfying the Chapman-Jouguet condition.

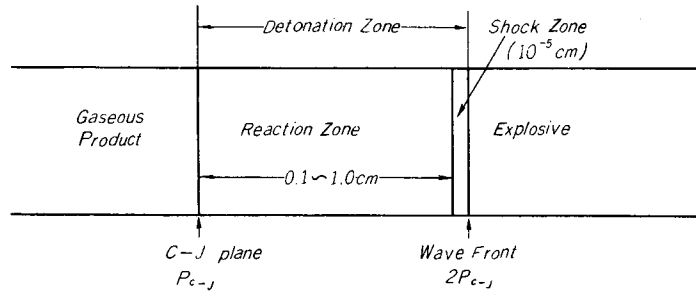


Fig. 17. Diagram of plane detonation wave.

the pressure becomes the stable detonation pressure (known as P_{C-J}) and the decomposition products reach the condition of thermal equilibrium. The width of the reaction zone has been considered to be of the order of 0.1 cm to 1 cm for the explosive compounds (TNT, Tetryl and etc.), and accordingly the reaction time becomes of the order of $0.2\mu\text{s}$ to $2\mu\text{s}$, assuming the velocity of detonation to be 5,000 m/s. The width of the reaction zone is influenced by the reaction velocity, and therefore the width of the reaction zone of industrial explosives is considered to be rather wider than that of the explosive compounds. Furthermore, it has been considered in the theory of detonation that the magnitude of pressure in the shock zone attains a value about twice as large as P_{C-J} , and moreover the pressure decreases to about one half of P_{C-J} when the particle velocity reduces to zero. This equalized pressure finally attained in a charge hole is usually denoted as P_{static} .

Accordingly, on account of the pressure increase produced at the attacked surface by the collision of the detonation wave against iron, as shown in Fig. 16, and the pressure increase at the shock zone which attains a magnitude twice as large as P_{C-J} , it is considered that the magnitude of the peak pressure produced at the attacked surface of iron by the impact of the detonation wave may reach a value of at least about $4P_{C-J}$.

Thus, by comparing the stress wave shape in the steel rod with the detonation wave shape, point (b) shown in Fig. 15 is supposed to be generated by the impact effect of the detonation wave front, and therefore the peak stress value at this point must amount to at least $4P_{C-J}$. Moreover, as P_{static} is believed to drop very slowly with the expansion and cooling of the produced gases, point (d) must correspond to the state of P_{static} . But the magnitudes of pressure at these points, of course, do not indicate directly the pressure in the detonation wave itself, because the pressure in the stress wave is expected to decay during its propagation through the gauge head.

Detonation Pressure produced at the Inner Surface of a Charge Hole

The direct measurement of the maximum detonation pressure acting on the inner surface of a charge hole in rock blasting is very difficult. However, the results obtained in the above experiments allow us to make certain inferences concerning that pressure.

The peak stress values in a steel rod at some distance from the attacked surface were measured in our present experiments and the results are shown in Tables 2 and 3. These peak stress values were plotted on logarithmic paper against the distance from the attacked surface as shown in Fig. 18. Referring to this figure, we can estimate the peak stress value near the attacked surface. Moreover, as has been explained previously, this peak stress value may be regarded as nearly equal to $4P_{C-J}$. In this way the pressure values of about 2×10^4 kg/cm² and 3×10^4 kg/cm² were estimated as the P_{C-J} -values corresponding to the velocities of detonation of 2,800 m/s and 3,300 m/s respectively.

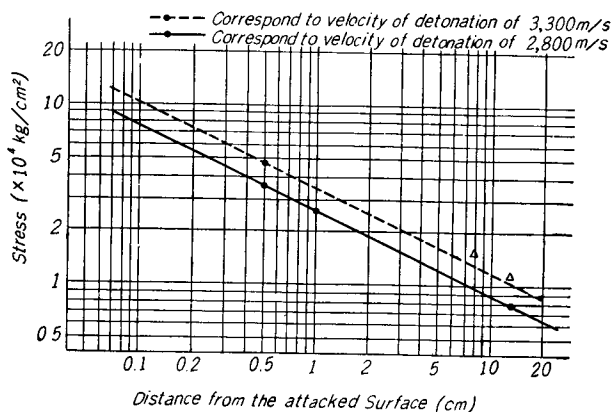


Fig. 18. Decay in stress due to distance in steel specimen.

On the other hand, the P_{C-J} -values and the velocities of detonation have been calculated for some kinds of explosives by J. Taylor⁷⁾. Of course the explosives selected by him have different compositions than the No. 3 Take dynamite used in our experiments. But the dynamic peak pressure at the C-J plane is considered to be rather more influenced by the velocity of detonation than by the composition of the explosive. Consequently if we compare our results with those calculated by Taylor, paying attention to the corresponding values of velocity of detonation, it will be found that the P_{C-J} -values estimated from our experiments are fairly reasonable.

Furthermore, it has been surmised from the results of the above experiments that the pressure acting on the inner surface of a charge hole rises very rapidly to its maximum value (within about $2\mu\text{s}$ or less), but this peak pressure falls quickly, and after about $15\mu\text{s}$, this pressure decreases to a value approximately that of P_{static} . The duration time of the detonation pressure in the charge hole was supposed to be about $500\mu\text{s}$ under the above experimental conditions, but in practice it may naturally be influenced by the amount of explosive, the effect of tamping, the state of failure, etc.

Acknowledgments

The authors' thanks are due to the authorities of the Kōmori mine, Nippon Kōgyo Co. Ltd., who kindly offered us a room for the present experiments in their underground openings.

The deep acknowledgments of the authors are made to Dr. T. Murata and Dr. T. Sakurai in the Taketoyo Plant of Nihon Yushi Co. Ltd. for their kind assistance in performing our auxiliary experiments on measuring the velocity of detonation of No. 3 Take dynamite.

References

- 1) I. Itō, M. Terada and T. Sakurai: THIS MEMOIRS, **22**, 13 (1960)
- 2) J. S. Rinehart: Jour. Appl. Phys., **22**, 555 (1951)
- 3) R. H. Cole: Underwater Explosions, Princeton University Press, (1948)
- 4) T. Hikita: Jour. Industrial Explosive Soc., Japan, **15**, 250 (1954)
- 5) I. Itō and T. Sakurai: Jour. Min. and Metall. Inst., Japan, **74**, 365 (1958)
- 6) F. W. Brown: Quarterly of the Colorado School of Mines, **51**, 171 (1956)
- 7) J. Taylor: Detonation in Condensed Explosives, Oxford Press, (1952)